

Wellesley College Wellesley College Digital Scholarship and Archive

Faculty Research and Scholarship

2013

Updates from the Dark Matter Time Projection Chamber Group (DMTPC)

James B.R. Battat
jbattat@wellesley.edu

Follow this and additional works at: <http://repository.wellesley.edu/scholarship>

Version: Publisher's version

Recommended Citation

Battat, J.B. R. [for the DMTPC Collaboration] "Updates from the Dark Matter Time Projection Chamber Group (DMTPC)." *Journal of Physics: Conference Series*, Volume 469, Issue 1, article id. 012001 (2013).

This Article is brought to you for free and open access by Wellesley College Digital Scholarship and Archive. It has been accepted for inclusion in Faculty Research and Scholarship by an authorized administrator of Wellesley College Digital Scholarship and Archive. For more information, please contact ir@wellesley.edu.

Updates from the Dark Matter Time Projection Chamber Group (DMTPC)

This content has been downloaded from IOPscience. Please scroll down to see the full text.

2013 J. Phys.: Conf. Ser. 469 012001

(<http://iopscience.iop.org/1742-6596/469/1/012001>)

View [the table of contents for this issue](#), or go to the [journal homepage](#) for more

Download details:

IP Address: 149.130.138.59

This content was downloaded on 17/03/2015 at 14:39

Please note that [terms and conditions apply](#).

Updates from the Dark Matter Time Projection Chamber Group (DMTPC)

James B. R. Battat [for the DMTPC Collaboration]

Wellesley College, Physics Department, 106 Central Street, Wellesley, MA 02481, USA

E-mail: jbattat@wellesley.edu

Abstract. The Dark Matter Time Projection Chamber (DMTPC) collaboration has developed a series of gas-based detectors with the goal of detecting the directional anisotropy of dark-matter-induced nuclear recoils. Here, we report on recent progress from the DMTPC group, focusing on the surface operation of the 4shooter detector.

1. Introduction

In early prototype detectors, the DMTPC collaboration demonstrated successful track reconstruction, including head/tail sensitivity, with CCD-based TPCs [6, 5]. Since then, the group has built and operated a 10-liter-volume detector, called the 10L. At the time, a surface run of that detector produced the most sensitive directional limit on the spin-dependent WIMP-proton cross-section [1]. Since then, the NEWAGE collaboration has matched this result (see NEWAGE contribution in this proceedings), and the DRIFT group have published a more sensitive limit [3]. The 10L detector has been relocated to an underground lab facility at the Waste Isolation Pilot Plant (WIPP) near Carlsbad, New Mexico (USA), and an underground run is currently underway.

In parallel with the 10L work, the DMTPC group designed and built a new detector called the 4shooter. The 4shooter is a modest scale-up of the 10L technology (by a factor of two in volume), with the goal of evaluating technologies and techniques that would be required for a cubic-meter DMTPC detector.¹ In particular, the 4shooter uses four CCD cameras to produce a mosaic image of the TPC amplification region. Also, in addition to the CCD readout, the 4shooter has both photomultiplier tube (PMT) and charge readout channels, with the goal of enhancing background rejection and 3D tracking capability.

In this work, we present recent results from the operation of the 4shooter detector at a surface laboratory at MIT (in Cambridge, MA, USA). In particular, we have characterized the gas gain, and calibrated the energy scale of the CCD and charge readout channels. In addition, we describe initial results on gamma background rejection, CCD track reconstruction techniques, and the head/tail reconstruction capability for low-energy (50–400 keV) alpha tracks.

¹ The cubic meter detector, named DMTPCino, has been funded for construction by NSF and DoE, and is currently under design by the DMTPC group.



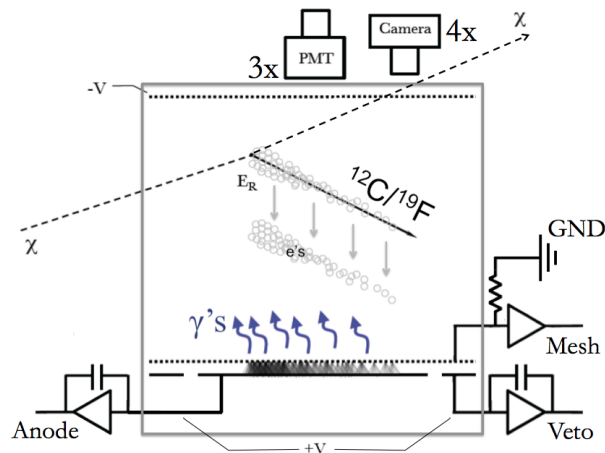


Figure 1. Schematic of the 4shooter detector showing a side-view of the TPC with mesh cathode ($-V$), mesh ground plane, and solid anode and veto electrodes ($+V$). A recoiling C or F nucleus ionizes the surrounding gas. Proportional amplification and scintillation light is produced in the mesh-anode gap (the amplification region). The charge signal is measured by the charge-integrating amplifiers on the anode and veto channels, as well as the high-bandwidth current amplifier on the mesh. The scintillation light is recorded by four CCD cameras and three photomultiplier tubes (PMT).

2. 4shooter Detector Hardware

As shown in Figure 1, the 4shooter detector is a time-projection chamber apparatus, housed within a vacuum chamber, with both charge and optical readout. The detector is filled with low-pressure CF_4 gas (45–75 Torr). The 26.7-cm tall drift region couples to a $420 \mu\text{m}$ tall amplification region through a stainless steel mesh that is common to both. Copper field shaping rings with 30.7 cm inner diameter provide a uniform drift electric field. The amplification region is a copper-clad G-10 plate with machined channels to define three separate electrodes: ground, anode and veto. The circular anode has a 29.2 cm diameter, and around the anode is an annular veto region of inner diameter 29.2 cm and outer diameter 30.7 cm. The veto channel is used for charge-based fiducialization in (x, y) . Finally, the remainder of the copper-clad G-10 plate (exterior to the veto), comprises the ground electrode, to which the amplification region mesh is epoxied. The total active volume of the detector is then defined by the drift length and the outer diameter of the veto channel, while the nominal fiducial volume (18 L) is set by the drift length and the outer diameter of the anode.

3. Gas gain

Measurements of the gas gain as a function of anode voltage and gas pressure were made using an ^{55}Fe source of 5.9 keV x-rays. As shown in Figure 2, at 75 Torr CF_4 , a gain of 10^5 was achieved (for an anode bias of 720 V). In standard operation, the detector is filled with 60 Torr CF_4 and the amplification region bias is 670 V. The resulting gas gain is 6.3×10^4 .² Additionally, the gas gain as a function of time was found to degrade by 3% but then stabilize over a 24 hour period. This behaviour is well-documented in gas detectors, and may be caused by the formation of hydrocarbon polymers on the anode [7].

We also found that the measured gas gain decreased with the rate of the ^{55}Fe source, likely due to space-charge formation in the amplification region [2]. We attenuated the source until the measured gas gain plateaued. Measurements of the gas gain with the unattenuated source

² Note, that we have assumed a W -value of 34 eV for CF_4 , though conflicting values appear in the literature (34 eV [10] and 54 eV [11]).

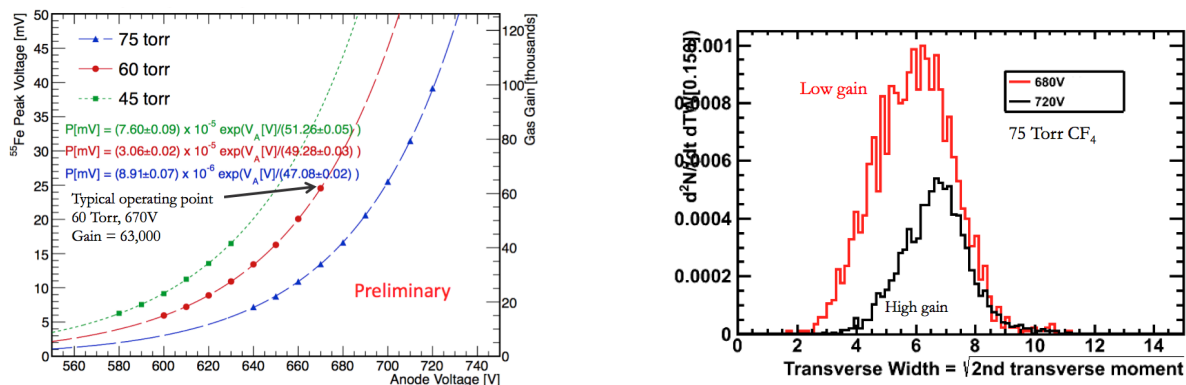


Figure 2. (Left): Gas gain as a function of anode voltage for three different CF₄ gas pressures. (Right): Distributions of transverse widths of neutron-induced nuclear recoils showing the absence of low-diffusion tracks at high detector gas gain, likely due to the Raether limit.

were 30% lower than with the attenuated source.

With the 4shooter detector, there is a high premium on gas gain, as the CCD acceptance is only 8×10^{-4} . But the trade-off of increasing the anode voltage to achieve a large gas gain is non-trivial. First, the rate of spontaneous discharges (sparks) increases. This reduces detector live-time and can lead to residual (ghost) images in subsequent CCD exposures. Second, the ionization density from a nuclear recoil, when amplified, may exceed 10^7 electrons (the so-called Raether limit), which can lead to event-triggered discharges. Particularly troublesome is the drift-distance dependence of the charge density (due to diffusion). For example, in Figure 2, we compare the transverse widths of neutron-induced nuclear recoil tracks in the CCD (the transverse width is correlated with the electron diffusion). We find that data at 75 Torr CF₄ and a high-gain setting (720V on the anode) shows an absence of low-diffusion tracks, while data at a lower gain (680V on the anode) shows the expected width distribution. A likely explanation is that the detector is blind to short-drift events at high gain because they trigger discharges in the amplification region due to Raether's criteria. During normal operations, we do not operate near the Raether limit.

4. CCD energy calibration

The energy scale of the CCDs is calibrated by comparing the longitudinal projection of ²⁴¹Am alpha particle tracks in each CCD field of view with Monte Carlo simulations (see Figure 3). The Monte Carlo parameters include the starting location of the source (tuned to match the mean range of the data), the electron diffusion (tuned to match the widths of the transverse projections of the tracks), the (negligible) gas quenching factor (using the parameterization of [5]), the CCD length scale (conversion from pixels to millimeters – obtained via independent measurements), the CCD noise per pixel (also obtained via independent measurements), as well as the desired parameter, the CCD conversion gain in units of ADU/keV_{ee} (where ADU are the Arbitrary Digital Units reported by the CCD).

An example of the agreement between the data and Monte Carlo is shown in Figure 3. The resulting CCD energy calibration parameters for 60 Torr CF₄ and anode voltage of 670 V are 10.3, 18.4, 18.6 and 16.6 ADU/keV_{ee} (all ± 0.2 ADU/keV_{ee}). The difference between the energy scale of the first CCD and the other three is due to a difference in the electron conversion gain (e⁻/ADU).

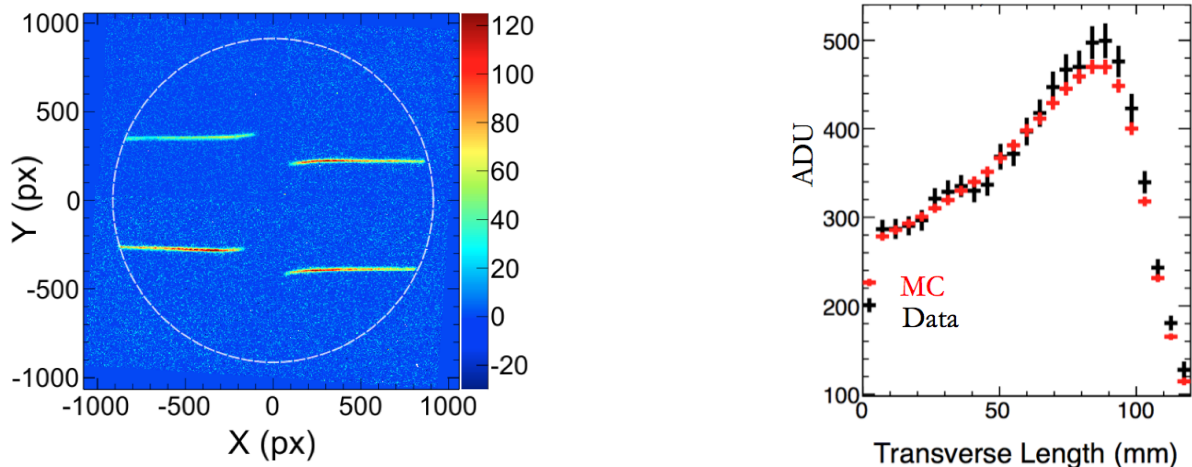


Figure 3. (Left): Mosaic image of the CCD energy calibration data showing a single alpha calibration source in the field of view of each CCD. The white dotted line marks the location of the inner diameter of the field-shaping rings onto which the alpha sources are mounted. (Right) The longitudinal projection of the average of many alpha tracks in a single CCD field of view for data (black) and Monte Carlo (red), showing good agreement between the two. The normalization of the Monte Carlo gives the CCD energy calibration in $\text{ADU}/\text{keV}_{ee}$.

5. Other results

The signal from the current amplifier attached to the amplification region mesh provides gamma background rejection via pulse shape discrimination. For example, with a similar detector (same amplification region geometry, but shorter drift region), the DMTPC group previously demonstrated a combined CCD/charge gamma rejection factor of 1.1×10^{-5} [8]. Although the background rejection factor has not yet been quantified on the 4shooter, the preliminary results suggest that we will achieve even better performance than in [8].

Additionally, a new approach to track reconstruction that employs a physical model for the nuclear stopping has been implemented. This approach not only leads to better track reconstruction accuracy, but also allows for the assignment of confidence/quality to each fit parameter, allowing for subsequent analyses to employ this confidence parameter. Two different fitting approaches have been developed: one-dimensional fits to the transverse and longitudinal projections of the 2D tracks in the CCD image, as well as a 2D fit to the original 2D track in the CCD image. Preliminary results of this work were presented recently at the TAUP 2013 conference [4].

Finally, we used an alpha source of known orientation situated outside of the drift region, oriented so that only the final 50–300 keV of the track penetrated through the cathode into the drift region. It was therefore possible to quantify the ability of the detector to correctly reconstruct the head-tail signature of low-energy ionization tracks. These tracks differ from the expected WIMP-induced nuclear recoils in two important ways. First, they are produced by alpha particles (not F recoils), so the track lengths are longer (optimistic), but the stopping (dE/dx) is smaller (pessimistic) than F recoils of the same energy. Second, the primary ionization is generated near the cathode, and so these events all travel the full 26.7 cm drift length of the detector and suffer the maximum diffusion (pessimistic). The promising initial results [9] show that the head-tail was measured correctly on 60% of tracks with energy between 60 and 80 keV. In the range of 100 to 120 keV, that fraction improved to 70%, and at 200 keV the fraction was 90%. Furthermore, the head-tail correct fraction is significantly increased with the use of the 2D track-fitting analysis described above [4].

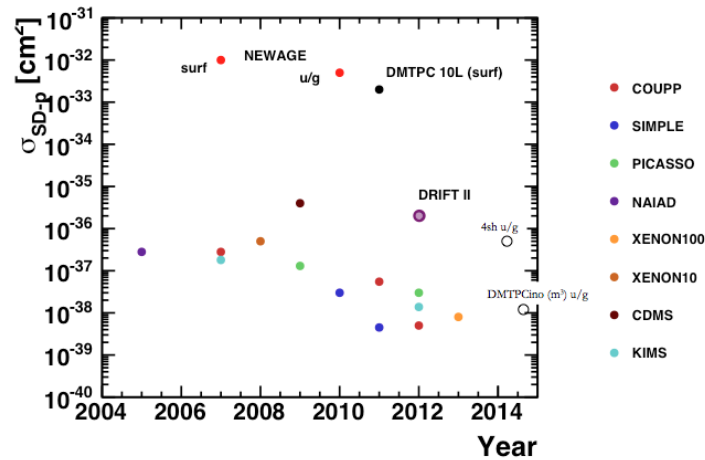


Figure 4. Limits on the spin-dependent WIMP-proton cross-section over time for both directional (DMTPC, DRIFT, NEWAGE) and non-directional detectors (listed in legend at right). The point labeled “4sh u/g” is the exclusion limit achievable if the 4shooter detector is operated background-free for one year with a 50 keV_r threshold. The corresponding sensitivity of the cubic-meter DMTPCino is also shown.

6. Projected sensitivity

The evolution over time of spin-dependent WIMP-proton cross-section limits is presented in Figure 4. Over the past seven years, the limits have improved by two orders of magnitude. The sensitivity of the 4shooter and the cubic-meter DMTPCino detector are also shown.

References

- [1] [DMTPC Collaboration] Ahlen, S. First dark matter search results from a surface run of the 10-L DMTPC directional dark matter detector. *Phys. Lett. B*, 695:124–129, January 2011.
- [2] A. Bressan et al. High rate behavior and discharge limits in micro-pattern detectors. *Nucl. Instrum. Meth.*, A424:321–342, March 1999.
- [3] E. Daw et al. Spin-dependent limits from the DRIFT-IIid directional dark matter detector. *Astropart. Phys.*, 35:397–401, February 2012.
- [4] [DMTPC Collaboration] Deaconu, C. Recent Updates from the Dark Matter Time Projection Chamber (DMTPC) Collaboration. In *13th International Conference on Topics in Astroparticle and Underground Physics (TAUP 2013)*, 2013.
- [5] [DMTPC Collaboration] Dujmic, D. Charge amplification concepts for direction-sensitive dark matter detectors. *Astropart. Phys.*, 30:58–64, 2008.
- [6] [DMTPC Collaboration] Dujmic, D. Observation of the “head-tail” effect in nuclear recoils of low-energy neutrons. *Nucl. Instrum. Meth.*, A592:123, 2008.
- [7] J. Kadyk. Gaseous Detectors - Novel Tracking Detectors. <http://www-group.slac.stanford.edu/sluc/lectures/Detector-Lectures.html>, October 1998. Accessed 2013-09-22.
- [8] [DMTPC Collaboration] Lopez, J. P. Background Rejection in the DMTPC Dark Matter Search Using Charge Signals. *Nucl. Instrum. Meth.*, A696:121–128, 2012.
- [9] [DMTPC Collaboration] Lopez, J. P. Updates from the DMTPC Dark Matter Search. American Physical Society April 2013 meeting, April 2013.
- [10] G. F. Reinking, L. G. Christophorou, and S. R. Hunter. Studies of total ionization in gases/mixtures of interest to pulsed power applications. *J. Appl. Phys.*, 60:499–508, July 1986.
- [11] A. Sharma. Properties of some gas mixtures used in tracking detectors. *SLAC-JOURNAL-ICFA-16-3*, July 1998.